Journal of Biomolecular NMR **29:** 85–90, 2004.

Solution structures of reduced and oxidized bacteriophage T4 glutaredoxin

Yunjun Wang, Godwin Amegbey & David S. Wishart*
Department of Computing Science and Biological Sciences, University of Alberta, Edmonton, T6G 2E8, Canada

Received 3 September 2003; Accepted 25 November 2003

Key words: glutaredoxin, NMR, protein, structure, T4 phage

Biological context

Glutaredoxins (Grx) are small, ubiquitous, structurally conserved family of proteins typically containing fewer than one hundred amino acids. They have been identified and sequenced in essentially all classes of organisms, including bacteriophage, bacteria, yeast, plants, invertebrates and mammals (Holmgren et al., 1999). All glutaredoxins characterized to date contain a common dithiol/disulfide redox active-site motif composed of four critical residues: C-[PV]-[FYW]-C. The glutaredoxins were initially discovered as hydrogen donors for ribonucleotide reductase, a key enzyme in DNA synthesis. Other biological functions of glutaredoxins include the catalysis of dehydroascorbate to ascorbate, the reactivation of DNA-binding activity of certain nuclear factors, the acceleration of in vitro protein folding rates and the regulation and/or maintenance of HIV-1 protease activity (Holmgren et al., 1999). Glutaredoxins share many structural and functional similarities to another important member of the thioltransferase superfamily – the thioredoxins (Trx). However, thioredoxins and glutaredoxins carry out their respective redox activities using fundamentally different mechanisms. In particular, the thioredoxin system uses NADPH, thioredoxin reductase, and thioredoxin; while the glutaredoxin system uses NADPH, glutathione reductase, glutathione, and glutaredoxin.

While sequence comparisons suggest that bacteriophage T4 glutaredoxin (T4 Grx) belongs to the glutaredoxin family, its level of sequence similarity to any other glutaredoxin rarely exceeds 20%. Furthermore, T4 glutaredoxin is the only glutaredoxin with a valine substitution of proline in the highly conserved second position of the C-P-[FYW]-C active site motif. These global and local sequence differences likely contribute to its unusual dual redox functionality as well. Recent experiments have shown that T4 Grx can be reduced not only by thioredoxin reductase but also by glutathione (Nikkola et al., 1993). Indeed, it was because of this functional hybridism that T4 glutaredoxin was originally known as bacteriophage T4 thioredoxin. It is only recently that this protein has become formally known as T4 glutaredoxin (Nikkola et al., 1991).

While several X-ray structures of oxidized T4 Grx (both native and mutant forms) have been reported, as yet no structure of the reduced form of the wild type protein has been determined. Similarly, no solution structure or NMR assignments for the oxidized form have been reported. This has limited our understanding of the structure/activity of this protein and the possible origins of its dual thioredoxin/glutaredoxin activity. Here we wish to describe the determination of the solution structures of wild-type T4 Grx in both the oxidized and reduced forms. We also describe the results of structural comparisons between both redox forms and related X-ray structures.

Methods and results

Sample preparation

T4 glutaredoxin was expressed in *E. coli* and purified using well established protocols previously described (LeMaster and Richards, 1988). While modest yields (15 mg/L) of T4 Grx were obtainable when cells were grown in rich (LB) media, attempts to prepare ^{15}N and ^{13}C labeled material in isotopically enriched minimal media were unsuccessful. Consequently all studies were conducted with unlabelled material. For the NMR experiments described here, a lyophilized T4 Grx sample was dissolved in a pH 6.0 buffer con-

*To whom correspondence should be addressed. E-mail: david.wishart@ualberta.ca

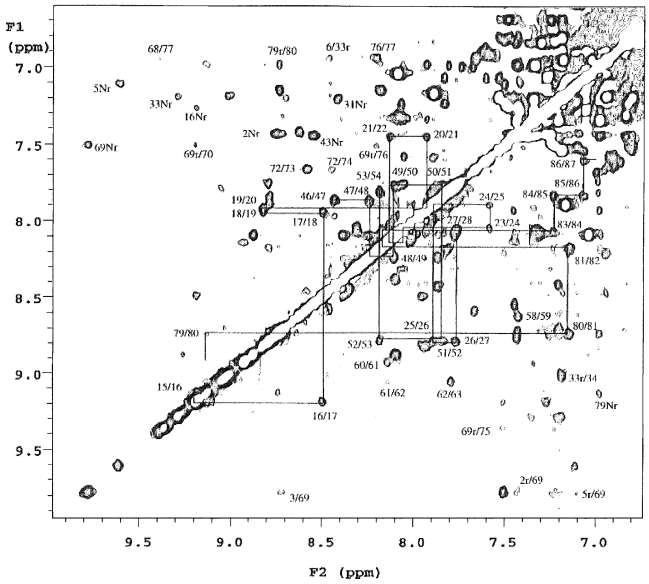

Figure 1. 1 H^N and aromatic region of the NOESY spectrum of oxidized T4 Grx. 'N' denotes amide proton, 'r' denotes aromatic ring proton and 'Nr' denotes an intra-residue amide/ring proton interaction.

taining 20 mM potassium phosphate and 150 mM NaCl in 99.99% D_2O or 90%H_2O/10%D_2O, yielding a final protein concentration of 2–3 mM. A small quantity (0.1 mM) of DSS was added to all samples as a chemical shift reference. The reduced form of T4 Grx was prepared by adding excess (10 mM) dithiothreitol (DTT) to the NMR sample after which it was blanketed with argon for 30 min and then sealed with an airtight rubber septum.

All ^{1}H NMR experiments were performed on Varian Unity 600 MHz and VXR 500 MHz NMR spectrometers equipped with 5-mm triple resonance probes. TOCSY experiments were carried out with mixing times ranging from 50 to 100 milliseconds. NOESY spectra were collected with mixing times ranging from 75 to 150 milliseconds. Phase-sensitive DQF-COSY spectra were also collected to facilitate stereo-specific assignments. Complete ^{1}H NMR chemical shift assignments were carried out manually using well-established procedures (Wüthrich, 1986). The ^{1}H NMR chemical shift assignments for the reduced and oxidized T4 Grx have been deposited into the BioMagResBank (accession numbers 4458 and 4459 respectively). Side chain χ_1 torsion angles and stereo-specific methylene assignments were extracted from DQF-COSY and NOESY spectra. $^3J_{HNH\alpha}$ coupling constants were obtained using line-width measurements from both TOCSY and NOESY spectra (Wang et al., 1997). Inter-proton distance restraints were derived from the assigned NOE peaks of NOESY spectra acquired with mixing times of 75, 100 and 150 milliseconds. The assigned NOE intensities (measured by volume integration) were classified into four groups: strong, medium, weak and very weak, corresponding to inter-proton distance restraints of 1.8–2.8 Å, 1.8–4.0 Å, 1.8–5.0 Å and 1.8–6.0 Å respectively. Upper distance limits for distances involving methyl protons and non-stereospecifically assigned methylene protons were corrected for center averaging. Backbone Φ torsion angles restraints were derived from $^3J_{HNH\alpha}$ coupling constants. Specifically; for those residues in well-defined β-sheet regions ($^3J_{HNH\alpha} > 8.5$ Hz), Φ angle restraints were set to $-120 \pm 30°$; for those residues in well defined helical regions, Φ angles were estimated from an appropriately parameterized Karplus equation (Wang and Bax, 1996) and assigned an uncertainty of $\pm$ 15°. Backbone ψ dihedral angle restraints were obtained from an analysis of dNα/dαN ratios (Gagné et al., 1994). Side chain χ_1 torsion angles constraints from DQF-COSY and NOESY spectra were set to 180°, $-60°$ or 60° with an uncertainty of $\pm$ 30°. Each hydrogen bond was defined using two distance restraints, $d_{O\text{-}H} = 1.8$–2.4 Å and $d_{O\text{-}N} = 2.7$–3.5 Å.

Simulated annealing protocols as implemented in the X-PLOR package (Brunger, 1992) were used for structural generation. In the calculation, 1050 distance restraints, 46 Φ angle restraints, 56 ψ angle

Table 1. Structural statistics for each ensemble of 30 structures calculated for both oxidized and reduced T4 glutaredoxin

Total restraints used	*Oxidized*	*Reduced*
Distance restraints (Å)	1050	1065
Dihedral angle restraints (°)	188	188
$^3J_{HNH\alpha}$ coupling constants restraints (Hz)	66	66
^{1}H chemical shift restraints (ppm)	201	201
RMSD from experimental restraints		
Distance (Å)	0.04 ± 0.01	0.04 ± 0.01
Dihedral angle (°)	0.23 ± 0.04	0.25 ± 0.04
$^3J_{HNH\alpha}$ coupling constants (Hz)	0.15 ± 0.06	0.17 ± 0.07
^{1}H chemical shift (ppm)	0.31 ± 0.10	0.28 ± 0.12
Deviations from idealized covalent geometry		
Bond distance (Å)	0.0036 ± 0.0011	0.0034 ± 0.0012
Bond angles (°)	0.51 ± 0.02	0.49 ± 0.05
Improper dihedral angles (°)	0.43 ± 0.05	0.38 ± 0.04
PROCHECK assessment		
Residues in most favored Φ/ψ regions (%)	82.1 ± 2.4	83.2 ± 2.2
Residues in additional allowed Φ/ψ regions (%)	16.5 ± 3.0	15.1 ± 2.9
Residues in generously allowed Φ/ψ regions (%)	1.4 ± 1.7	1.6 ± 1.8
Residues in disallowed Φ/ψ regions (%)	0	0
Hydrogen bond energy (Kcal/mol)	0.78 ± 0.08	0.81 ± 0.10
Van der Waals energy (Kcal/mol)	−349.4 ± 38.4	−351.1 ± 33.4
Number of bad contacts/100 residues	1.9 ± 1.2	2.1 ± 1.4
Atomic RMSD to the average structure		
Backbone atoms (Å)	0.71 ± 0.10	0.70 ± 0.11
All heavy atoms (Å)	1.27 ± 0.11	1.28 ± 0.12
Atomic RMSD to the X-ray structure (1ABA)		
Backbone atoms (Å)	1.40 ± 0.13	1.39 ± 0.16
All heavy atoms (Å)	2.34 ± 0.20	2.36 ± 0.21
Atomic RMSD of average structure to the X-ray structure (1ABA)		
Backbone atoms (Å)	1.21	1.23
All heavy atoms (Å)	1.96	2.01

restraints, 86 ω angle restraints, 13 χ_1 angle restraints, 66 $^3J_{HNH\alpha}$ coupling constant restraints, and 201 ^{1}H chemical shift restraints were used in the calculation for the oxidized protein. The numbers of constraints used for the reduced form were approximately the same as for the oxidized form (given the high overall spectral similarity). Of the 50 NMR structures calculated for each redox form, a subset of 30 structures satisfied the criteria of lowest energy and was accepted into the final ensemble. The quality of the final ensemble of structures was assessed with PROCHECK NMR (Laskowski et al., 1996). The coordinates were deposited into the Protein Data Bank (PDB) under accession numbers 1DE1 and 1DE2 for the oxidized and reduced forms respectively. The parameters and structural statistics determined with the PROCHECK NMR program (see Table 1) indicate that the quality of our T4 Grx NMR structures is comparable to a 2.0 Å X-ray structure. The backbone RMSD is just 0.71 Å for the oxidized form and 0.70 Å for the reduced form. These RMSD values fall to just 0.59 Å and 0.60 Å when residues in the flexible loops (9-14, 56-63, and 71-73) are excluded from the calculation.

Discussion and conclusions

Both the reduced and oxidized forms of T4 Grx contain three α-helices extending from residues 14 to 27, 44 to 55, and 78 to 86. A portion of NOESY spectrum of the oxidized T4 Grx showing the $d_{NN[i,i+1]}$ connectivity in these helices is presented in Figure 1. In the center of the molecule is a well-defined four-strand β-sheet. The first β-strand (β_1) extends from residues 2 to 7, the second (β_2) from 30 to 36, the

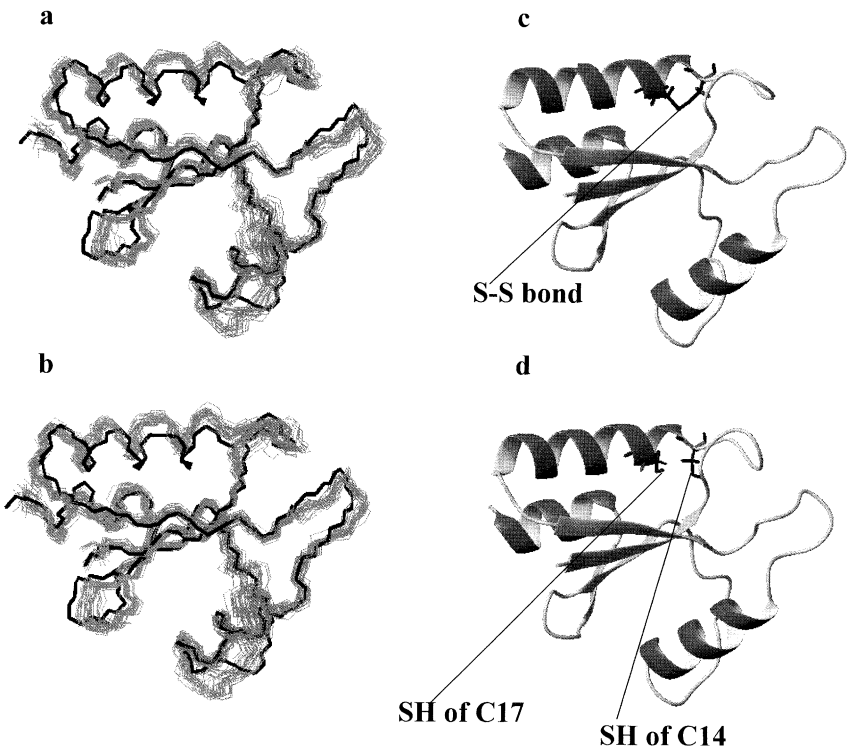

Figure 2. Superposition of the 30 lowest energy structures of (a) oxidized and (b) reduced T4 glutaredoxin showing the backbone atoms. The backbone of the T4 Grx X-ray structure (1ABA) is shown as a thick dark line in each ensemble. Ribbon diagrams of the final restrained minimized mean structures of (c) oxidized and (d) reduced T4 glutaredoxin showing the side chains of residues C14 and C17.

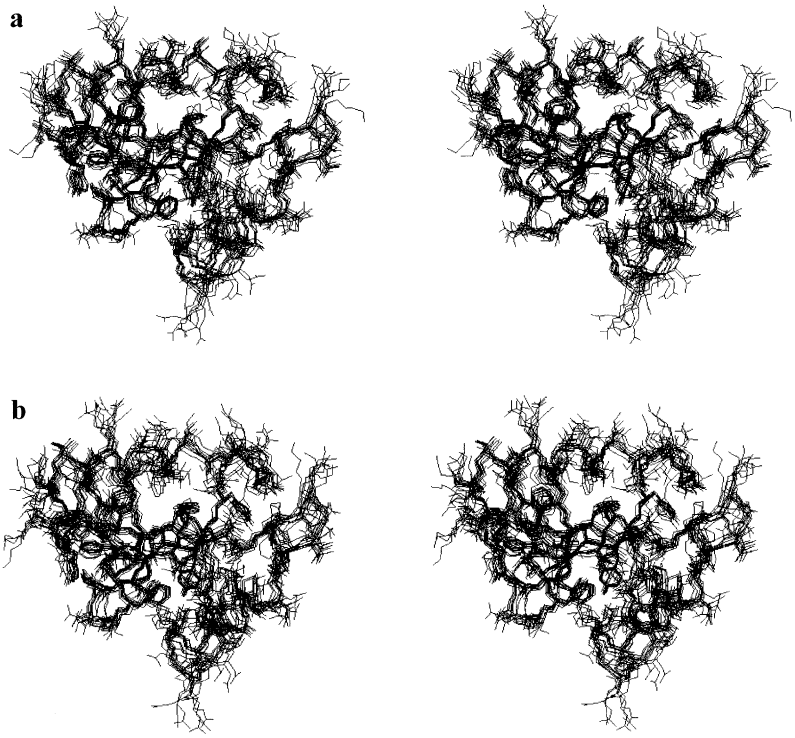

Figure 3. Stereoviews of the NMR structural ensemble, including side chains of (a) oxidized and (b) reduced T4 Grx.

third (β_3) from 64 to 70 and the fourth (β_4) from 73 to 77. Ribbon diagrams along with superimposed backbone traces of the final ensemble of 30 optimized structures of both reduced and oxidized T4 Grx are shown in Figure 2. The redox-active site (Cys14-Val15-Tyr16-Cys17) is located on the N-terminal side of the first helix. Close inspection of the active site structure shows that the side-chains of Tyr7, Tyr16 and Met65 effectively block any approaches to Cys17. On the other hand, Cys14 remains partly exposed in both oxidized and reduced T4 Grx. As with all other thioredoxins and glutaredoxins, T4 Grx has a *cis* proline located near its active site. The *cis* configuration of the Met65-Pro66 peptide bond, which is present in both oxidized and reduced T4 Grx, was easily identified from the characteristic $d_{\alpha\alpha[i,i+1]}$ NOE connectivities seen in our NOESY spectra.

Careful comparison between these two structures as well as additional comparisons between the observed NOE connectivities, $^3J_{HNH\alpha}$ coupling constants, chemical shifts and location of slowly exchanging amide protons reveals a very high degree of similarity between reduced and oxidized T4 Grx. Superposition of the two redox forms yields an RMSD of only 0.63 Å for the backbone atoms and 1.45 Å for all heavy atoms. This observation is consistent with an earlier X-ray crystallographic study of an active site T4 Grx mutant (Val15-Gly and Tyr16-Pro) that showed only minor structural perturbations occurring after reduction of the disulfide bond (Ingelman et al., 1995). This is also consistent with NMR data previously reported for the oxidized and reduced forms of related thiol-transferases (Nordstrand et al., 2000).

Although a high level of structural similarity exists for both oxidized and reduced T4 Grx, there are at least two notable differences. The first and most obvious difference concerns the active site loop. The loss of the disulfide bond in the reduced form clearly leads to greater flexibility in this loop relative to the oxidized form. This is manifested in a number of ways, including narrower line widths, changes in amide shifts and J-coupling constants towards random coil values, greater average Sγ separation between Cys14 and Cys17 (4.05 Å vs. 2.02 Å) and increased dispersion of the two cysteine side chains (Figures 2 and 3). While somewhat imprecisely measurable in the reduced form, the degree of Sγ separation is consistent with data obtained for other members of the glutaredoxin/thioredoxin family. In particular, the distance between the Cys23 Sγ and Cys26 Sγ atoms in reduced human Grx (1JHB) was found to be 4.1 Å while the distance between the Cys32 Sγ and Cys35 Sγ atoms in reduced *E. coli* Trx (1XOB) was measured at 3.8 Å. The second significant difference between reduced and oxidized T4 Grx concerns their chemical shifts ($^1H\alpha$ and ^1HN) and coupling constants ($^3J_{HNH\alpha}$). The reduction of T4 Grx leads to moderate (>0.1 ppm) $^1H\alpha$ chemical shift changes for a number of residues spatially proximal to the redox active site. These include Gly6, Tyr7, Val15, Tyr16, Cys17, Asp18, Asn19, Asn35, Ile36, Thr64, Gln67, His75 and Gly78. Even larger chemical shift changes (>0.3 ppm) are observed for amide protons belonging to Tyr7, Cys14, Val15, Ile36, Gln60, Met65 and His75. Visual comparisons, distance measurements and chemical shift calculations using SHIFTX (Neal et al., 2003) indicate that the α-protons of both Tyr7 and Asn35 are influenced by Phe33, while the α-protons of Asn19 and His75 are affected by Phe79 and Phe69, respectively.

Comparison of the NMR T4 Grx structures to the 1.45 Å X-ray structure (1ABA) of an active-site T4 Grx mutant reported by Eklund et al. (1992) reveals that the backbone atomic RMSD between each restraint-minimized NMR structure and the X-ray structure is 1.40 Å for the oxidized form, and 1.39 Å for the reduced form (Table 1). While the overall folds of both NMR structures and the X-ray structure are very similar, some differences exist between them especially in the active site and the 56-61 loop regions. Eklund et al. (1992) found that the Sγ atoms of Cys14 and Cys17 in the active-site mutant of reduced T4 Grx were separated by just 2.03 Å – some 2.0 Å less than what we have measured for wild-type reduced T4 Grx. In the 56-61 loop region the solution structure is not particularly well-defined due to a low 'density' of constraints. The X-ray structure clearly indicates that the side-chains of Leu51 and Leu52 in helix α_2 should be quite close (<5 Å) to the side-chains of Arg57, Thr59 and Asn60 in this particular loop. However, no such interaction could be found in NOESY spectra collected with a variety of different mixing times.

Nearly two dozen three-dimensional structures of thioredoxins and glutaredoxins have been reported over the past 25 years. To assess the similarities and differences between T4 Grx and other Grx/Trx relatives we chose to compare the atomic structures of eight evolutionary distinct members of the thioredoxin/glutaredoxin superfamily (*E. coli* Trx, *E. coli* Grx 1, *E. coli* Grx 3, human Trx, human Grx, porcine Grx, *M. thermoautotrophicum* Trx (Mt0807) *and Anabaena sp* Trx-2 to our NMR structures of

T4 Grx. The backbone superposition of the four-stranded β-sheet for all nine highly divergent proteins (minimum pairwise sequence identity <15%) yields a RMSD value of only 1.32 Å. This level of conservation is quite remarkable and it suggests that the central β-sheet scaffold must play a key role in the folding and stability of all members of this ubiquitous family of proteins. In addition to the high level of structural conservation seen in the central β-sheet, there is also an equally high level of structural conservation in their active site loops. A backbone superimposition of the Cys-Xaa-Xaa-Cys redox active site (oxidized) for all nine glutaredoxin / thioredoxin molecules yields an RMSD value of just 0.36 Å. This high level of structural similarity in both thioredoxin and glutaredoxin active sites indicates just how precise the backbone geometry must be in order to confer the redox activity seen in this class of proteins. While the active site loop is structurally well conserved, it is important to emphasize that the character and disposition of side chains around this active site is not. The nature and consequences of these differences significantly affects the biochemical properties of these proteins. In particular, a relatively low pKa (<5.0) has been predicted for the most solvent exposed cysteine (Cys14) of T4 Grx based on data collected for other glutaredoxins (Eklund et al., 1992). However, the pKa for Cys14 as determined by Wang (1999) is actually 6.8. This unusually high pKa indicates that T4 Grx has an active site titration chemistry that is actually more akin to a thioredoxin than a glutaredoxin. The low pKa values normally seen for glutaredoxins appear to arise from the presence of a large, positive local electrostatic potential. Inspection of the structures of the active site regions of T4 Grx, *E. coli* Trx and porcine Grx as well as their immediate surroundings indicates there are relatively few basic amino acids near the *E. coli* Trx and T4 Grx thiols, but substantially more basic (positively charged) residues surround the active site thiols in porcine Grx. The large, local positive electrostatic potential in porcine Grx (and the low pKa – 3.8, for its nucleophilic Cys) likely arises from the proximity to five positively charged residues: Lys19, Agr26, Lys27, Arg67, and Arg71, all of which are highly conserved in the glutaredoxin family. On the other hand, T4 Grx only has two positively charged residues (His12 and Lys13) close to the redox-active site. Since histidine can only be positively charged at low pH values, it is unlikely to affect the ionization of a thiol at neutral pH. Consequently this paucity of positive charge at the active site of T4 Grx could account for the unusually high pKa of Cys14.

To summarize, we have determined the NMR assignments and solution structures for both reduced and oxidized T4 Grx. The availability of these NMR results may open the way to more detailed studies and a better understanding of the dual redox character of T4 Grx. They may also suggest ways of engineering multiple activities into other thioredoxins or glutaredoxins.

Acknowledgements

The authors wish to thank David M. LeMaster, Kathy Borden, Frederic M. Richards and Brian D. Sykes for their advice and assistance during the very early phases of this project. Financial support by the NSERC (Canada) is gratefully acknowledged. Y.W. was supported by a PMAC-MRC postgraduate scholarship.

References

Brunger, A.T. (1992) *X-PLOR Version 3. 1. A System for X-Ray Crystallography and NMR*, Yale University Press, New Haven, CT.

Eklund, H., Ingelman, M., Söderberg, B.-O., Uhlin, T., Nordlund, P., Nikkola, M., Sonnertam, U., Joelson, T. and Petratos, K. (1992) *J. Mol. Biol.*, **228**, 596–618.

Gagné, S.M., Tsuda, S., Li, M.X., Chandra, M., Smillie, L.B. and Sykes, B.D. (1994) *Protein Sci.*, **3**, 1961–1974.

Holmgren, A., Arnér, E.S.J. and Berndt, K.D. (1999) Glutaredoxin, In *The Encyclopedia of Molecular Biology*, Creigthon, T.E. (Ed.), John Wiley and Sons, Inc. New York, pp. 1020–1023.

Ingelman, M., Nordlund, P. and Eklund, H. (1995) *FEBS Lett.*, **370**, 209–211.

Laskowski, R.A., Rullman, J.A.C., MacArthur, M.W., Kaptein, R. and Thornton, J. (1996) *J. Biomol. NMR*, **8**, 477–486.

LeMaster, D.M. and Richards, F.M. (1988) *Biochemistry*, **27**, 142–150.

Neal, S., Nip, A.M., Zhang, H. and Wishart, D.S. (2003) *J. Biomol. NMR*, **26**, 215–240

Nikkola, M., Gleason, F.K. and Eklund, H. (1993) *J. Biol. Chem.*, **268**, 3845–3849.

Nikkola, M., Gleason, F.K., Saarinen, M., Joelson, T., Björnberg, O. and Eklund, H. (1991) *J. Biol. Chem.*, **266**, 16105–16112.

Nordstrand, K., Sandström, A., Åslund, F., Holmgren, A., Otting, G. and Berndt, K.D. (2000) *J. Mol. Biol.*, **303**, 423–432.

Wang, C.A. and Bax, A. (1996) *J. Am. Chem. Soc.*, **118**, 2483–2494.

Wang, Y. (1999), Ph.D Thesis, University of Alberta, Edmonton, Alberta.

Wang, Y., Nip, A.M. and Wishart, D.S. (1997) *J. Biomol. NMR*, **10**, 373–382.

Wüthrich, K. (1986) *NMR of Proteins and Nucleic Acids*, Wiley Inter-Science, New York.